CHAPTER IV

EFFECTS OF NUCLEATING AGENTS ON CRYSTALLIZATION AND MELTING BEHAVIOR AND MECHANICAL PROPERTIES OF NUCLEATED SYNDIOTACTIC POLYPRORYLENE

ABSTRACT

The effects of various nucleating agents [e.g. 1,3:2,4-dibenzylidene sorbitol (DBS), 1,3:2,4-di-*p*-methyldibenzilidene sorbitol (MDBS), 1,3:2,4-di-*m*,*p*-methylbenzylidene sorbitol (DMDBS), kaolin, talcum, marl, titanium dioxide (TiO_2), and silica (SiO_2)] on non-isothermal melt-crystallization and subsequent melting behavior and mechanical properties of nucleated syndiotactic polypropylene (sPP) in comparison with those of the neat sample were investigated. Analysis of the non-isothermal melt-crystallization exotherms revealed that the ability for these fillers in nucleating sPP could be ranked from the best to the worst as follows: DBS > talcum > MDBS > kaolin > SiO_2 > DMDBS > marl > TiO_2. Analysis of the subsequent melting endotherms revealed that most of the sPP compounds exhibited double melting peaks, while only marl-filled sPP exhibited triple melting peaks and that the stability of the primary crystals for all of the sample types investigated can be ranked from the best to the worst in the following order: DBS-filled > talcum-filled > MDBS-filled ~ DMDBS-filled ~ kaolin-filled > SiO_2-filled > marl-filled > TiO_2-filled > neat sPP samples. Wide-angle X-ray diffraction analysis showed that addition of these fillers did not affect the modification of the sPP crystals. Mechanical property measurements revealed that both of the tensile strength and the percentage of elongation at yield for sPP compounds investigated were not much different from those of the neat sPP. After natural weathering for 1 month, the tensile strength at yield for sPP compounds investigated increased, at the expense of the percentage of elongation at yield, but, after natural weather for 3 months, both of the tensile strength and the percentage of elongation at yield were found to decrease.

(**Key-words**: syndiotactic polypropylene; crystallization; nucleation; mechanical properties)

1. INTRODUCTION

Syndiotactic polypropylene (sPP) of high regio- and stereo-regularities was successfully synthesized by Ewen et al. [1] using a metallocene catalytic system, instead of the traditional Ziegler-Natta catalytic system [2]. This led to renewed interests in this polymer [3-8]. Despite some of its interesting properties, such as high ductility and high optical transparency, the syndiotactic form of PP (i.e. sPP) has enjoyed less commercial success than its isotactic counterpart (iPP) [9].

Among a number of drawbacks, the slow crystallization rate of sPP is an important factor limiting commercial utilization of this polymer [10]. Studies related to crystallization process of semi-crystalline polymers are of great importance in polymer processing, because the resulting physical properties of the products are strongly related to the extent of crystallization and the morphology formed. Both the quiescent isothermal and non-isothermal melt-crystallization studies revealed that sPP is a slowly crystallizing polymer [10,11]. Addition of nucleating agents may help enhance the crystallization rates by providing more sites for nucleation, hence reducing the cycle time.

Nucleating agents can be either inorganic or organic in their chemical makeup. Some examples for inorganic nucleating agents are talcum, mica, barium sulfate ($BaSO_4$), and calcium carbonate ($CaCO_3$); whereas, some examples for organic ones are sorbitals and their derivatives. Typically, $CaCO_3$ is added to isotactic polypropylene (iPP) to reduce the cost of the final product, to improve mechanical properties (e.g. modulus and heat stability), and to enhance crystallization rate. To our knowledge, the only available reports on filled systems in sPP have been concerned with the mechanical and thermal properties, including phase behavior, of sPP filled with glass beads and talcum [12-14] and with the effects of $CaCO_3$ of various sizes and surface treatments on thermal and mechanical properties of sPP/$CaCO_3$ compounds [15].

The present contribution is aimed at studying the effects of some organic nucleating agents (i.e. DBS, MDBS, and DMDBS) and some inorganic nucleating agents [i.e. kaolin, talcum, marl, titanium dioxide (TiO_2) and silicon dioxide (SiO_2)] on non-isothermal melt-crystallization and subsequent melting behavior and mechanical properties of sPP compounds in comparison with neat sPP. The effect of

natural weathering of up to three months on mechanical properties of neat sPP and sPP filled with talcum, marl, and TiO_2 was also investigated.

2. EXPERIMENTAL DETAILS

2.1. Materials

Syndiotactic polypropylene (sPP) used in this work was produced and supplied by AtoFina Petrochemicals (USA) based on a metallocene technology. Some physical properties of the resin, reported by the manufacturer, are density = 0.88 $g \cdot cm^{-3}$ (ASTM D1505), melt flow index = 2 g/10 min (ASTM D1238), tensile strength at yield = 15 MPa (ASTM D638), tensile modulus = 480 MPa (ASTM D638), percentage of elongation at yield = 11% (ASTM D638), flexural modulus = 340 MPa (ASTM D790), and notched Izod impact strength = 640 $J \cdot m^{-1}$ (ASTM D256A).

Inorganic fillers used in this work are kaolin [$Al_2Si_2O_5(OH)_4$; Engelhard Corporation (USA)], talcum [$Mg_3Si_4O_{10}(OH)_2$, Pacific Commo Trading (Thailand)], marl [$CaSiO_3$; Pacific Commo Trading (Thailand)], titanium dioxide [TiO_2; Pacific Commo Trading (Thailand)], and SiO_2 [PPG Siam Silica (Thailand)]. Organic fillers are some sorbitol derivatives such as 1,3:2,4-dibenzylidene sorbitol [DBS; Ciba Specialty Chemicals (Switzerland)], 1,3:2,4-di-*p*-methyldibenzilidene sorbitol [MDBS; Ciba Specialty Chemicals (Switzerland)], and 1,3:2,4-di-*m,p*-methylbenzylidene sorbitol [DMDBS; Milliken Asia (Singapore)]. The average particle size of these fillers was measured by a Malvern Instruments Masterizer X particle size analyzer was found to be the followings (in descending order): marl = 42.5 ± 2.0 μm, SiO_2 = 36.4 ± 0.7 μm, DBS = 26.8 ± 1.0 μm, kaolin = 15.1 ± 1.5 μm, talcum = 13.9 ± 1.8 μm, DMDBS = 6.7 ± 0.6 μm, TiO_2 = 5.3 ± 1.0 μm, and MDBS = 5.3 ± 0.6 μm.

2.2. Sample preparation

All of the fillers used were first dried in a hot-air oven at 60°C for 14 hrs and then cooled down to room temperature. Each filler was then dry-mixed with sPP pellets in a tumble mixer for 10 min and later compounded in a Collin ZK25 self-

wiping, co-rotating twin-screw extruder, operating at a screw speed of 50 rpm and the die temperature of 190°C. Due to the limitation on the amount of sPP resin and fillers in possession, only 5 percent by weight (wt.%) of each inorganic filler or 1 wt.% of each organic filler was added to the sPP resin. A Planetrol 075D2 pelletizer was used to palletize the extrudate after coming out of the twin-screw kneader.

A film of each compound was prepared by melt-pressing sliced pellets between a pair of transparency films, which were sandwiched between a pair of stainless steel platens in a Wabash V50H compression press. The temperature of the platens was set at 190°C. The molding was pre-heated for 5 min, before compressing under an applied clamping force of 10 tons for another 5 min. Later, the film was cooled down, while still in the compression machine, until the temperature of the platens read 40°C. Each film specimen was used for studying non-isothermal crystallization and subsequent melting behavior.

An ARBURG Allrounder® 270M injection molding machine was used to prepare specimens for tensile and impact tests. The operation settings of the injection molding machine were as the followings: barrel temperature = 195°C, nozzle temperature = 200°C, mold temperature = 50°C, clamping force = 25 kN, and injection pressure = 1,000 bars. Tensile and impact specimens were prepared according to ASTM D638-91 and ASTM D256-90b standard test methods, respectively. Prior to corresponding mechanical tests, both of the tensile and impact specimens were conditioned at ambient condition for 3 days. Some specimens made out of neat sPP and sPP filled with talcum, marl, and TiO_2 were subjected to natural weathering over the periods of 1 and 3 months prior to mechanical tests.

2.3. Differential scanning calorimetry measurements

Non-isothermal melt-crystallization and subsequent melting behavior of neat sPP and sPP filled with various organic and inorganic nucleating agents were investigated on a Perkin-Elmer Series7 differential scanning calorimeter (DSC). Temperature calibration was performed on every other run using a pure indium standard (T_m^0 = 156.6°C and ΔH_f^0 = 28.5 J·g^{-1}). Each sample of 6.0 ± 0.5 mg in weight, cut from the as-prepared films, was sealed in an aluminum sample holder.

The experimental procedure started with heating each sample from 25 to 190°C using a heating rate of 80°C·min^{-1} in order to set a similar thermal history to all the samples studied. After melt-annealing period of 5 minutes at 190°C, the sample was cooled down at a cooling rate of 10°C·min^{-1} to 25°C in order to observe non-isothermal melt-crystallization behavior. As soon as the program temperature reached 25°C, the sample was immediately reheated at a heating rate of 20°C·min^{-1} in order to observe the subsequent melting behavior. Both non-isothermal crystallization exotherm and subsequent melting endotherm were recorded for further analysis. It is important to note that each sample was used only once and all of the runs were carried out under nitrogen atmosphere.

2.4. Crystal structure and crystallinity measurement

A Rigaku Rint2000 wide-angle X-ray diffractometer (WAXD) was used to determine the crystal modification and apparent degree of crystallinity of both neat sPP and sPP compounds which were non-isothermally melt-crystallized at a cooling rate of 10°C·min^{-1} in DSC (viz. each sample was cooled from 190 to 25°C without the subsequent heating scan). The X-ray source was operated at a voltage of 40 kV and a filament current of 30 mA to generate CuK_α radiation (λ = 1.54 Å). The scanning range covered the scattering angles 2θ in the range of 5 to 50°.

2.5. Mechanical property measurements

The tensile strength at yield, percentage of elongation at yield, and Young's modulus for both neat sPP and sPP compounds were measured on an Instron 4206 universal testing machine according to ASTM D638-91 standard test method using a 100 kN load cell and a 50 mm·min^{-1} crosshead speed. Izod impact resistance of these specimens was determined on a Swick 5113 impact tester according to ASTM D256-90b standard test method using a 2.7 Joule pendulum and a 124.4° release angle. The hardness of the surface of these specimens was measured on a Matsuzawa DXT-3 Rockwell hardness tester according to ASTM D785 standard test method using scale-R. The results from these tests were reported as averages of the data taken from at least 10 specimens.

2.6. Microstructural observation

A JEOL 520-2AE scanning electron microscope (SEM) was used to observe the microstructure of the impact-fractured surface of selected specimens obtained after impact testing. Each selected specimen was cut about 2 mm below the fractured surface and the cut piece was stuck onto an aluminum stub. Prior to observation under SEM, each sample was gold-coated to enhance the conductivity of the surface.

3. RESULTS AND DISCUSSION

3.1. Non-isothermal melt-crystallization and subsequent melting behavior

Figure 1 illustrates non-isothermal melt-crystallization exotherms, recorded at a cooling rate of 10°C/min, for neat sPP and sPP filled with various inorganic (i.e. kaolin, talcum, marl, TiO_2, and SiO_2) and organic (i.e. DBS, MDBS, DMDBS) fillers. For most sample types, a single crystallization exotherm was observed, while sPP filled with kaolin, marl, and SiO_2, interestingly, showed another exotherm located at a high temperature region. Since the temperature range where the high-temperature exotherm was observed was too high to be assigned as the crystallization of the primary crystals formed during a cooling scan, only the low-temperature one was considered in this work. Obviously, incorporation of these fillers, though in a very small amount (i.e. 5 wt.% for inorganic fillers and 1 wt.% for organic fillers), was able to shift the crystallization exotherm towards a higher temperature from that of neat sPP. Among the exotherms shown, the non-isothermal crystallization exotherm of DBS-filled sPP sample was found to locate in the highest temperature range, followed by that of talc-filled, MDBS-filled, DMDBS-filled, kaolin-filled, SiO_2-filled, marl-filled, TiO_2-filled, and neat sPP samples, respectively. According to the results shown in Figure 1, it can be concluded based on the fillers used and the conditions studied in this work that DBS was the best, while TiO_2 was the worst, nucleating agent for sPP.

In order to quantify the non-isothermal melt-crystallization data obtained, some characteristic parameters are defined, viz. T_{ch} = the temperature at the maximum crystallization rate or the peak temperature of the high-temperature exotherm (for sPP filled with kaolin, marl, and SiO_2), $T_{0.01}$ = the temperature at 1%

relative crystallinity, T_{cl} = the temperature at the maximum crystallization rate or the peak temperature of the crystallization exotherm (for neat sPP and sPP filled with other fillers excepted for kaolin, marl, and SiO_2) or the low-temperature crystallization exotherm (for sPP filled with kaolin, marl, and SiO_2), and $T_{0.99}$ = the temperature at 99% relative crystallinity. $T_{0.01}$ and $T_{0.99}$ are used here to represent the beginning and the ending of the non-isothermal melt-crystallization process. The values of these parameters for all of the sample types investigated are summarized in Table 1. Generally, the position of the non-isothermal melt-crystallization exotherm can be used to judge the ability of a filler in nucleating the matrix polymer. According to the $T_{0.01}$ values shown in Table 1, the ability of these fillers in nucleating sPP can be ranked in the following order: DBS > talcum > MDBS > kaolin > SiO_2 > DMDBS > marl > TiO_2, while it is DBS > talcum > MDBS > DMDBS > kaolin > SiO_2 > marl > TiO_2, when judging from the T_{cl} values.

In an attempt to quantify the nucleation ability of these fillers on sPP, some characteristic parameters are defined, viz. $\Delta T_{0.01}$ = the difference between the $T_{0.01}$ values of an sPP compound and the neat sPP and ΔT_{cl} = the difference between the T_{cl} values of an sPP compound and the neat sPP. The calculated $\Delta T_{0.01}$ and ΔT_{cl} for the data shown in Table 1 are as follows: for DSB-filled sPP, they are 17.9 and 18.6°C; for MDBS-filled sPP, they are 15.2 and 16.8°C; for DMDBS-filled sPP, they are 12.0 and 16.0°C; for kaolin-filled sPP, they are 14.4 and 15.8°C; for talcum-filled sPP, they are 15.8 and 17.6°C; for marl-filled sPP, they are 8.2 and 12.8°C; for TiO_2-filled sPP, they are 5.9 and 9.5°C; and for SiO_2-filled sPP, they are 13.4 and 14.3°C. Based on these values, the nucleation ability among these fillers can be ranked from best to worst as follows: DBS > talcum > MDBS > kaolin > SiO_2 > DMDBS > marl > TiO_2 (when judging from the $\Delta T_{0.01}$ values) or DBS > talcum > MDBS > DMDBS > kaolin > SiO_2 > marl > TiO_2 (when judging from the ΔT_{cl} values).

After non-isothermal melt-crystallization at 10°C·min^{-1}, each sample was immediately reheated at a heating rate of 20°C·min^{-1} to 180°C to observe the subsequent melting behavior (see Figure 2). Clearly, at this cooling rate, all of the sample types investigated exhibited double melting peaks, with an exception to the subsequent melting thermogram of sPP filled with marl which exhibited triple

melting peaks. The occurrence of the middle-temperature melting peak in marl-filled sPP was not known at this point. Generally, the position and the relative size of the two endotherms among these sample types were found to be different from one another. In order to quantify the subsequent melting behavior of these sample types, some characteristic parameters are defined, viz. T_{ml} = the peak temperature of the low-temperature melting endotherm, T_{mh1} = the peak temperature of the high-temperature melting endotherm (for neat sPP and sPP filled with other fillers excepted for marl), T_{mh2} = the peak temperature of the middle-temperature melting endotherm (for sPP filled with marl). The values of these parameters for all of the sample types investigated are summarized in Table 2.

It was shown previously [16] that the low-temperature melting endotherm corresponded to the melting of the primary crystals formed, thus the position and sharpness of this endotherm should correlate with the position of the crystallization exotherm. If T_{cl} is used to represent the stability of the primary crystals formed during non-isothermal cooling (see Table 1), the stability of the primary crystals of all of the sample types investigated should be in the following order: DBS-filled > talcum-filled > MDBS-filled > DMDBS-filled > kaolin-filled > SiO_2-filled > marl-filled > TiO_2-filled > neat sPP samples. It is generally known that crystals of greater stability should melt at a higher temperature. According to the the T_{ml} data summarized in Table 2, the stability of the primary crystals of all of the sample types studied can be ranked in the following sequence: DBS-filled > talcum-filled > MDBS-filled ~ DMDBS-filled ~ kaolin-filled > SiO_2-filled > marl-filled > TiO_2-filled > neat sPP samples, which is in excellent agreement with the observation obtained earlier based on the T_{cl} data.

In an attempt to further quantify the subsequent melting behavior of these samples, some characteristic parameters are defined, viz. ΔT_{ml} = the difference between the T_{ml} values of an sPP compound and the neat sPP and ΔT_{mh1} = the difference between the T_{mh1} values of an sPP compound and the neat sPP. The calculated ΔT_{ml} and ΔT_{mh1} for the data shown in Table 2 are summarized as follows: for DSB-filled sPP, they are 8.1 and 3.2°C; for MDBS-filled sPP, they are 6.7 and 2.0°C; for DMDBS-filled sPP, they are 6.7 and 2.1°C; for kaolin-filled sPP, they are

6.7 and 1.5°C; for talcum-filled sPP, they are 7.4 and 1.5°C; for marl-filled sPP, they are 5.7 and 2.1°C; for TiO_2-filled sPP, they are 3.7 and 1.2°C; and for SiO_2-filled sPP, they are 6.4 and 1.3°C. Obviously, the differences between the T_{mh1} values of various sPP compounds and the neat sPP were not so large as the differences between the T_{m1} values of various sPP compounds and the neat sPP. This experimental fact is quickly recognized since it was shown [16] that the high-temperature melting endotherm corresponded to the melting of the recrystallized crystals formed during a reheating scan and was found to less dependent on the crystallization temperature.

3.2. Crystal structure and apparent degree of crystallinity

In order to observe the crystal structure and the resulting apparent degree of crystallinity of neat sPP and sPP compounds investigated, WAXD technique was utilized. Figure 3 illustrates WAXD patterns for neat sPP and sPP filled with various inorganic and organic fillers. It should noted that each sample was prepared in the DSC cell by cooling at a rate of 10°C min^{-1} after melt-annealing at 190°C for 5 minutes. For neat sPP, the characteristic X-ray peaks were observed at the scattering angles 2θ of ca. 12.1, 15.8, 20.5 and 24.5°, corresponding to limit-disordered orthorhombic unit cell with axes a = 14.5 Å, b = 5.6 Å and c = 7.4 Å [17-20]. According to this unit cell, the characteristic X-ray peaks should be observed at the 2θ of ca. 12.2, 15.8, 20.8 and 24.5°, corresponding to the reflection planes of (200), (010), (111) and (400), respectively.

In case of sPP filled with organic fillers (see Figure 3a), only the characteristic X-ray peaks of the limit-disordered orthorhombic unit cell of sPP crystals were observed, with the peaks of being more pronounced than those of neat sPP. In case of sPP with inorganic fillers (see Figure 3b,c), there were characteristic X-ray peaks other than those of the limit-disordered orthorhombic unit cell of sPP crystals being observed. More specifically, for kaolin-filled sPP, an extra characteristic X-ray peak was observed at the 2θ of 23.7° (compared with the expected peaks of kaolin at the 2θs of 23.7, 25.3, and 66.4°, respectively [21]). For talcum-filled sPP, extra characteristic X-ray peaks were observed at the 2θs of 9.3,

28.5, 32.6, 38.4, and 48.5° (compared with the expected peaks of talcum at the 2θ's of 9.6, 28.7, 32.8, 38.6, and 48.8°, respectively [21]). For marl-filled sPP, extra characteristic X-ray peaks were observed at the 2θ's of 11.5, 18.0, 23.1, 25.2, 26.7, 28.7, 32.8, 35.0, 38.3, and 38.9° (compared with the expected peaks of marl at the 2θ's of 11.6, 12.0, 23.3, 25.4, 27.0, 29.0, 33.0, 35.2, 38.6, and 39.2°, respectively [21]). For TiO_2-filled sPP, extra characteristic X-ray peaks were observed at the 2θ's of 25.1, 36.8, 37.7, and 47.9° (compared with the expected peaks of TiO_2 at the 2θ's of 25.3, 27.4, 37.0, 37.8, 48.1, and 53.9°, respectively [21]). Lastly, for SiO_2-filled sPP, an extra characteristic X-ray peak was observed at the 2θ of 21.4° (compared with the expected peak of SiO_2 at the 2θ of 22.0° [21]).

The results shown in Figure 3 suggest that addition of these fillers did not alter the crystal modification of the sPP crystals. It did, however, affect the apparent degree of crystallinity ${\chi_c}^{WAXD}$ of the sPP crystals. For a WAXD pattern of a semicrystalline polymer, the ${\chi_c}^{WAXD}$ can be conveniently taken as the relative ratio between the integrated intensities under the crystalline peaks A_c and the integrated total intensities A_t (i.e. $A_t = A_c + A_a$, where A_a is the integrated intensities under the amorphous halo), viz.

$$\chi_c^{WAXD}(\%) = \frac{A_c}{A_c + A_a} \times 100 \in [0,100]. \qquad (1)$$

In order to calculate the ${\chi_c}^{WAXD}$ value for each sample type, the obtained WAXD pattern was deconvoluted by fitting all of the characteristic X-ray peaks observed to a Gaussian function. The calculated values of ${\chi_c}^{WAXD}$ for all of the sample types investigated are as follows: for neat sPP, it is 5.6%; for DBS-filled sPP, it is 9.6%; for MDBS-filled sPP, it is 7.7%; for DMDBS-filled sPP, it is 7.0%; for kaolin-filled sPP, it is 4.6%, for talcum-filed sPP, it is 20.7%, for marl-filled sPP, it is 5.0%; for TiO_2-filled sPP, it is 5.2%; and, lastly, for SiO_2-filled sPP, it is 6.9%, respectively. It should be noted that contribution from the characteristic peaks of inorganic fillers were excluded from the calculated ${\chi_c}^{WAXD}$ values for sPP filled with inorganic fillers. Obviously, the ${\chi_c}^{WAXD}$ values for most of the sPP compounds investigated did not differ much from that of the neat sPP, with the exception of that of the talcum-filled sPP which showed much increase in the ${\chi_c}^{WAXD}$ value.

3.3. Mechanical properties

3.3.1. Effect of different fillers

Due to some processing limitations, only neat sPP and sPP filled with DBS, MDBS, talcum, marl, and TiO_2 were tested for the mechanical properties. Tested values of the tensile strength at yield, percentage of elongation at yield, Young's modulus, notched Izod impact strength, and surface hardness (scale-R) for these sample types are summarized in Table 3. Clearly, the measured values of the mechanical properties of neat sPP were much greater than those reported by the manufacturer. According to the results shown in Table 3, it is evident that the tensile strength at yield and the percentage of elongation at yield of sPP compounds investigated were not much different from those of the neat sPP, which is most likely a result of the addition of the small amount of these filler. In case of the Young's modulus, both DBS-filled and MDBS-filled sPP was found to have a lower value, while talcum-filled and marl-filled sPP exhibited a higher value, than that of the neat sPP, that of the TiO_2-filled sPP was found to have a comparable value to that of the neat sPP.

The notched Izod impact resistance values of DBS-filled, MDBS-filled, and TiO_2-filled sPP were all found to be slightly lower, while those of talcum-filled and marl-filled sPP were found to be much lower, than that of the neat sPP. The main reason for such a reduction in the impact resistance due to the presence of these fillers may be the poor interfacial adhesion between the surface of the fillers and the sPP matrix. Upon failure, cracks tend to propagate along the weaker interfacial region, which does not offer resistance to crack propagation as effective as the polymer matrix, rather than through the polymer matrix [22]. According to Table 3, the values of the surface hardness of sPP compounds were not much different from that of the neat sPP, with the exception of that of talcum-filled sPP which showed a slight lower value than that of the neat sPP.

3.3.2. Morphology of fracture surface

SEM micrographs of the fracture surface of neat sPP and sPP filled with DBS, MDBS, talcum, marl, and TiO_2 are illustrate in Figure 4a to e, respectively. According to these micrographs, the presence of these fillers was not clearly

observed, due to the very small amount of the fillers added. As evident from some of the micrographs, the poor interfacial adhesion between the fillers and the sPP matrix was apparent with the smooth surface of the filler pull-out sites (e.g. see Figure 4d and e). The rough facture surface clearly observed in these micrographs also suggests that permanent plastic deformation was common among these sample types. The results confirm the ductility property of the sPP matrix.

3.3.3. Effect of natural weathering

Due to some limitations, only neat sPP and sPP filled with talcum, marl, and TiO_2 were tested for the effect of natural weathering on their mechanical properties. All of the specimens investigated were left on an open rooftop over the periods of 1 and 3 months. The result for each sample type and weathering condition was report as an average obtained from at least ten specimens and was compared with that of the unweathered specimen.

Figure 5 shows the tensile strength at yield, percentage of elongation at yield, Young's modulus, notched Izod impact strength, and surface hardness of neat sPP and some sPP compounds both before and after natural weathering. In the first month of weathering, the tensile strength at yield for all of the sample types investigated was found to increase, at the expense of the percentage of elongation at yield (see Figure 5a and b). During this first month, the thermal energy obtained from the sunlight may be responsible for rearranging the structure of the crystals already present in the samples, hence an increase in the apparent degree of crystallinity, without appreciable molecular degradation as a result of the exposure to ultraviolet rays. On the contrary, for specimens after three months of weathering, both the tensile strength and the percentage of elongation at yield were found to decrease, most likely due to extensive chain scission of the sPP molecules. Extensive chain scission causes structural damage to the tie chains and the entanglements, rendering a detrimental effect to the ductility of the polymer, as had been proven by several studies [23-27].

The Young's modulus of all the sample types investigated exhibited a similar behavior to the tensile strength at yield, in which, after one month of weathering, the Young's modulus for most of the sample types investigated was found to increase,

while, after three months of weathering, the Young's modulus was found to decrease (see Figure 5c). In case of the impact strength, all of the sample types investigated exhibited a monotonically decrease in its impact strength value from that of the neat condition with increasing weathering period from 1 to 3 months (see Figure 5d). A drastic decrease in the impact strength value was observed for sPP filled with TiO_2 after only one month of weathering, which may be owing to the fact that TiO_2 can catalytically enhance photo-degradation of the polymer molecules [28,29]. For longer period of weather, the further decrease in the impact strength may attribute to the formation of sub-surface cracks, causing the polymer to lose its toughness [30].

On the contrary to results on the impact strength, the surface hardness for all of the sample types investigated showed a monotonous increase in its value from that of the neat condition with increasing weathering period from 1 to 3 months (see Figure 5e). The enhancement in the surface hardness may result from an increase in the apparent degree of crystallinity, on one hand, and from densification of the samples, on the other. The increase in the apparent degree of crystallization can occur via rearrangement of the molecules in and around the crystalline region as a result of the increased kinetic energy when being exposed to sunlight. On the other hand, densification may occur as a result of the collapsing of the molecules in the amorphous region after they went through a photo-degradation process via chain scission. The shorter molecules with increased mobility can also contribute to the increase in the apparent degree of crystallinity. In addition, an increase in the number of polar groups as a results of oxidative degradation can also lead to further densification of the amorphous region [31].

4. CONCLUSIONS

The effects of various inorganic and organic nucleating agents [e.g. 1,3:2,4-dibenzylidene sorbitol (DBS), 1,3:2,4-di-*p*-methyldibenzilidene sorbitol (MDBS), 1,3:2,4-di-*m*,*p*-methylbenzylidene sorbitol (DMDBS), kaolin, talcum, marl, titanium dioxide (TiO_2), and silica (SiO_2)] on non-isothermal melt-crystallization and subsequent melting behavior and mechanical properties of nucleated syndiotactic polypropylene (sPP) in comparison with those of the neat sample were investigated and reported for the first time. Based on the values of the temperature at 1% relative

crystallinity, the ability for these fillers in nucleating sPP could be ranked from the best to the worst as follows: DBS > talcum > MDBS > kaolin > SiO_2 > DMDBS > marl > TiO_2. Qualitatively, DBS was able to shift the onset of the crystallization process of sPP by ca. 18°C, while TiO_2 was able to do so by only ca. 6°C. Most of the sPP compounds exhibited double melting peaks, while only sPP filled with marl exhibited triple melting peaks. Based on the values of the low-temperature melting endotherm, the stability of the primary crystals for all of the sample types investigated can be ranked from the best to the worst in the following order: DBS-filled > talcum-filled > MDBS-filled ~ DMDBS-filled ~ kaolin-filled > SiO_2-filled > marl-filled > TiO_2-filled > neat sPP samples. Wide-angle X-ray diffraction analysis revealed that addition of these fillers did not affect the modification of the sPP crystals. Mechanical property measurements revealed that both of the tensile strength and the percentage of elongation at yield for sPP compounds investigated were not much different from those of the neat sPP. After natural weathering for 1 month, the tensile strength at yield for sPP compounds investigated increased, at the expense of the percentage of elongation at yield, but, after natural weather for 3 months, both of the tensile strength and the percentage of elongation at yield were found to decrease.

ACKNOWLEDGEMENTS

The authors wish to thank David C. Anderson of ATOFINA Petrochemicals (USA) for supplying the sPP resin, Engelhard Corporation (USA) for supplying kaolin, Pacific Commo Trading (Thailand) for supplying talcum, marl, and titanium dioxide, PPG Siam Silica (Thailand) for supplying silica, Ciba Specialty Chemicals (Switzerland) for supplying DBS and MDBS, and Milliken Asia (Singapore) for supplying DMDBS. Partial supports received from the Petroleum and Petrochemical Technology Consortium (through a Thai governmental loan from the Asian Development Bank), Chulalongkorn University (through a grant from the Ratchadapisek Somphot Endowment Fund for the foundation of the Conductive and Electroactive Polymers Research Unit), and the Petroleum and Petrochemical College, Chulalongkorn University are gratefully acknowledged.

REFERENCES

[1] Ewen, J. A.; Johns, R. L.; Razavi, A.; Ferrara, J. D. J Am Chem Soc 1988, 110, 6255.

[2] Natta, G.; Pasquon, I.; Zambelli, A. J Am Chem Soc 1962, 84, 1488.

[3] Rodriguez-Arnold, J.; Bu, Z.; Cheng, S. Z. D. J Macromol Sci – Rev Macromol Chem Phys 1995, C35, 117.

[4] Schardi, J.; Sun, L.; Kimura, S.; Sugimoto, R. J Plastic Film Sheeting 1996, 12, 157.

[5] Sun, L.; Shamshoum, E.; Dekunder, G. SPE-ANTEC Proc 1996, 1965.

[6] Gownder M. SPE-ANTEC Proc 1998, 1511.

[7] Sura, R. K.; Desai, P.; Abhiraman, A. S. SPE-ANTEC Proc 1999, 1764.

[8] Guadagno, L.; Naddeo, C.; D'Aniello, C.; Maio, L.; Vitoria, V.; Acierno, D. Macromol Symp 2002, 180, 23.

[9] Loos, J.; Bonnet, M.; Petermann, J. Polymer 2000, 41, 351.

[10] Supaphol, P.; Spruiell J.E. J Appl Polym Sci 2000, 75, 44.

[11] Supaphol, P. J Appl Polym Sci 2000, 78, 338.

[12] Stricker, F.; Burch, M.; Mülhaupt, R. Polymer 1997, 38, 5347.

[13] Stricker, F.; Mülhaupt, R. Polym Eng Sci 1998, 38, 1463.

[14] Stricker, F.; Maier, R.-D.; Burch, M.; Thomann, R.; Mülhaupt, R. Polymer 1999, 40, 2077.

[15] Supaphol, P.; Harnsiri, W.; Junkasem, J. J Appl Polym Sci 2004, 92, 201.

[16] Supaphol, P. J Appl Polym Sci 2001, 82, 1083.

[17] Lovinger, A. J.; Lotz, B.; Davis, D. D.; Padden, F. J. Macromolecules 1993, 26, 3494.

[18] Auriemma, F.; De Rosa, C.; Corradini, P. Macromolecules 1993, 26, 5719.

[19] De Rosa, C.; Auriemma, F.; and Vinti, V. Macromolecules 1997, 30, 4137.

[20] De Rosa, C.; Talarico, G.; Caporaso, L.; Auriemma, F.; Galimberti, M.; Fusco, O. Macromolecules 1998, 31, 9109.

[21] http://www.webmineral.com

[22] Tjong, S. C.; Li, R. K. Y.; Cheung, T. Polym Eng Sci 1997, 37, 166.

[23] Tidjani, A. J Appl Polym Sci 1997, 64, 2497.

[24] Rabello, M. S.; White, J. R. J Appl Polym Sci 1997, 64, 2505.

[25] Mendes, L. C.; Rufino, E. S.; de Paula, F. O. C.; Torres Jr, A. C. Polym Degrad Stab 2003, 79, 371.

[26] Lyons, J.S. Polym Test 1998, 17, 237.

[27] O'Donnell, B.; Qayyum, M. M.; Tong, L.; White, J. R. Plas Rubber Compos Proc Appl 1994, 21, 297.

[28] Allen, N. S.; Edge, M. in Fundamental of Polymer Degradation and Stabilisation. Chichester. Chapman and Hall, 1992.

[29] Allen, N. S.; Katami, H.; Thompson, F. Eur Polym J 1992, 28, 817.

[30] Leong, Y. W.; Abu Baker, M. B.; Mohd Ishak, Z. A.; Ariffin, A. Polym Degrad Stab 2004, 83, 411.

[31] Taveres, A. C.; Gulmine, J. V.; Lepienski, C. M.; Akcelrud, L. Polym Degrad Stab 2003, 81, 367.

CAPTION OF TABLES

CAPTION OF FIGURES

Figure1 Non-isothermal melt-crystallization exotherms of neat sPP and all of the sPP compounds for a fixed cooling rate of $10°C \cdot min^{-1}$.

Figure 2 Subsequent melting endotherms (recorded at a fixed heating rate of $20°C \cdot min^{-1}$) or neat sPP and all of the sPP compounds after non-isothermal melt-crystallization for a fixed cooling rate of $10°C \cdot min^{-1}$.

Figure 3 WAXD patterns for (a) neat sPP and sPP filled with DBS, MDBS, DMDBS; (b) neat sPP and sPP filled with kaolin, marl, SiO_2, and TiO_2; and (c) neat sPP and sPP filled with talcum.

Figure 4 SEM micrographs of fracture surfaces of (a) neat sPP, (b) DBS-filled sPP, (c) MDBS-filled sPP, (d) talcum-filled sPP, (e) marl-filled sPP, and (f) TiO_2-filled sPP.

Figure 5 (a) Tensile strength at yield, (b) percentage of elongation at yield, (c) Young's modulus, (d) notched Izod impact strength, and (e) surface hardness (scale-R) of neat sPP and sPP filled with talcum, marl, and TiO_2.

Table 1. Characteristics of non-isothermal melt-crystallization observed for all of the sample types investigated

Sample	Crystallization Characteristics				
	T_{ch} (°C)	$T_{0.01}$ (°C)	T_{cl} (°C)	$T_{0.99}$ (°C)	ΔH_c (J g^{-1})
neat sPP	-	76.0	64.1	58.4	28.5
DBS-filled sPP	-	94.0	82.7	72.2	21.5
MDBS-filled sPP	-	91.2	80.9	68.6	22.1
DMDBS-filled sPP	-	88.1	80.0	72.4	21.5
kaolin-filled sPP	115.3	90.5	79.9	71.4	18.0
talcum-filled sPP	-	91.8	81.7	72.7	16.8
marl-filled sPP	110.2	84.3	76.9	69.7	15.6
TiO_2-filled sPP	-	81.9	73.6	66.5	26.4
SiO_2-filled sPP	115.0	89.5	78.4	68.2	20.9

Table 2. Characteristics of subsequent melting behavior observed for all of the sample types investigated

Sample	Subsequent Melting Characteristics				
	T_{ml} (℃)	T_{mh1} (℃)	T_{mh2} (℃)	ΔH_{ml} ($J\ g^{-1}$)	ΔH_{mh} ($J\ g^{-1}$)
neat sPP	111.3	124.0	-	16.5	17.1
DBS-filled sPP	119.4	127.3	-	28.4	4.5
MDBS-filled sPP	118.0	126.0	-	29.3	6.0
DMDBS-filled sPP	118.0	126.1	-	24.6	6.4
kaolin-filled sPP	118.0	125.5	-	27.4	10.5
talcum-filled sPP	118.7	125.5	-	24.9	5.0
marl-filled sPP	117.0	126.1	122.7	26.9	12.1
TiO_2-filled sPP	115.0	125.2	-	10.5	29.5
SiO_2-filled sPP	117.7	125.3	-	24.1	8.9

Table 3. Mechanical properties observed for all of the sample types investigated

Samples	Tensile Strength at Yield (Mpa)		Percentage of Elongation at Yield (%)		Young's Modulus (Mpa)		Impact Strength (J/m)		Hardness (scale-R)	
	Mean	S.D.	Mean	S.D.	Mean	S.D.	Mean	S.D.	Mean	S.D.
neat s-PP	17.69	0.49	13.72	0.59	639.80	113.68	688.59	38.12	58.50	4.40
DBS-filled sPP	17.76	0.33	14.41	0.65	588.76	70.27	671.83	15.72	57.01	2.19
MDBS-filled sPP	17.75	0.46	14.63	0.65	592.79	32.59	665.26	23.82	58.28	2.32
talcum-filled sPP	17.86	0.52	13.51	0.42	663.01	81.24	147.92	9.30	53.17	3.88
marl-filled sPP	17.46	0.46	14.03	0.38	768.24	111.71	133.67	11.01	57.17	4.32
TiO_2-filled sPP	18.01	0.35	14.03	0.62	623.48	60.57	616.71	21.86	56.44	3.71

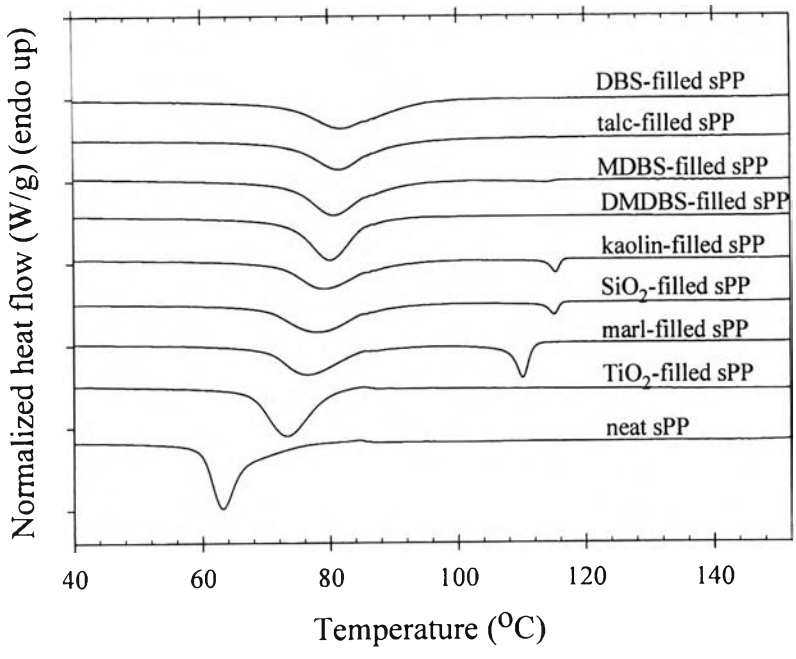
Normalized heat flow (W/g) (endo up)
DBS-filled sPP
talc-filled sPP
MDBS-filled sPP
DMDBS-filled sPP
kaolin-filled sPP
SiO2-filled sPP
marl-filled sPP
TiO2-filled sPP
neat sPP
40
60
80
100
120
140
Temperature (°C)

Figure 1

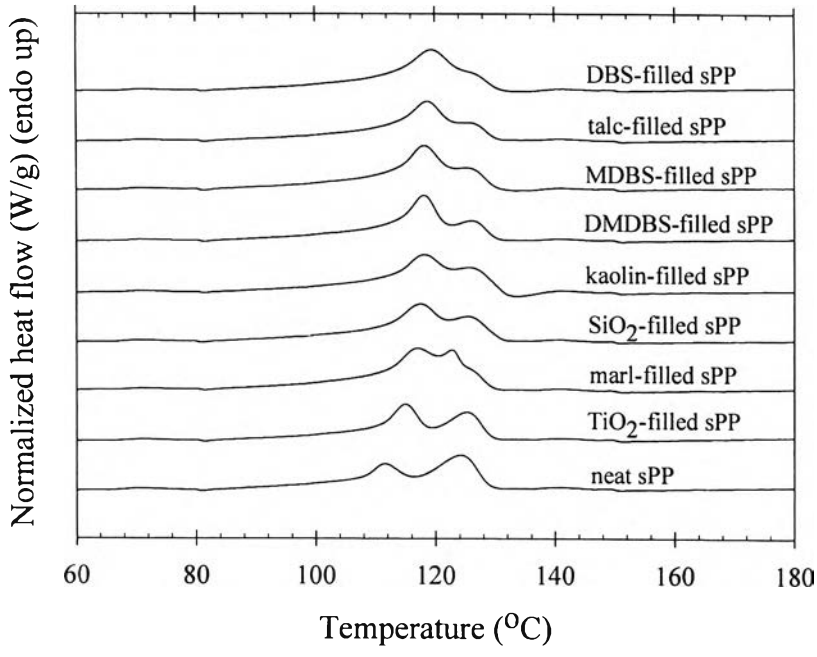
Normalized heat flow (W/g) (endo up)
DBS-filled sPP
talc-filled sPP
MDBS-filled sPP
DMDBS-filled sPP
kaolin-filled sPP
SiO2-filled sPP
marl-filled sPP
TiO2-filled sPP
neat sPP
60
80
100
120
140
160
180
Temperature (°C)

Figure 2

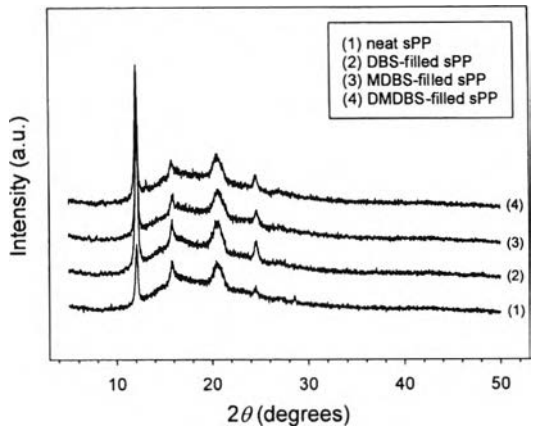
(1) neat sPP
(2) DBS-filled sPP
(3) MDBS-filled sPP
(4) DMDBS-filled sPP
Intensity (a.u.)
(4)
(3)
(2)
(1)
10
20
30
40
50
2θ (degrees)

(a)

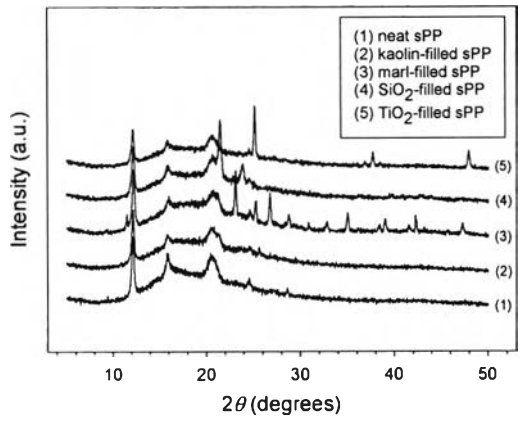
(1) neat sPP
(2) kaolin-filled sPP
(3) marl-filled sPP
(4) SiO2-filled sPP
(5) TiO2-filled sPP
Intensity (a.u.)
(5)
(4)
(3)
(2)
(1)
10
20
30
40
50
2θ (degrees)

(b)

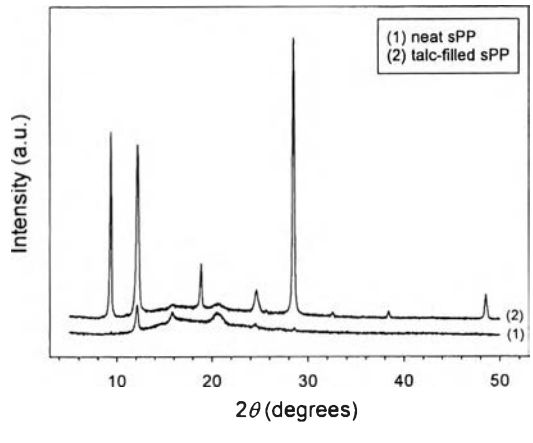
(1) neat sPP
(2) talc-filled sPP
Intensity (a.u.)
(2)
(1)
10
20
30
40
50
2θ (degrees)

(c)

Figure 3

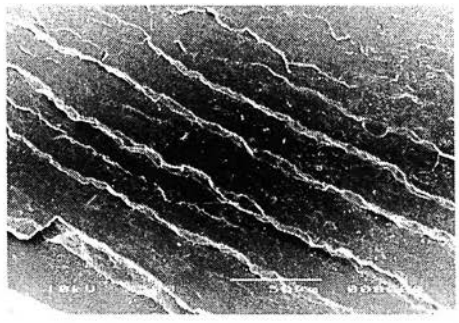

(a)

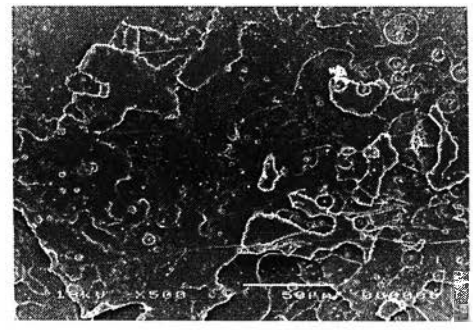

(b)

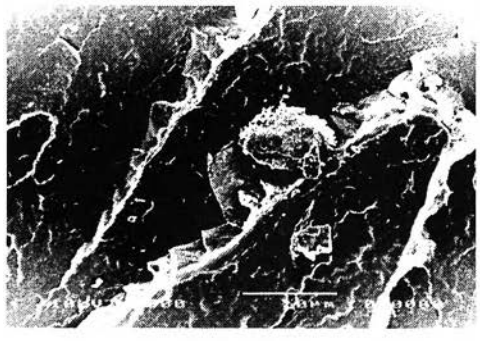

(c)

(d)

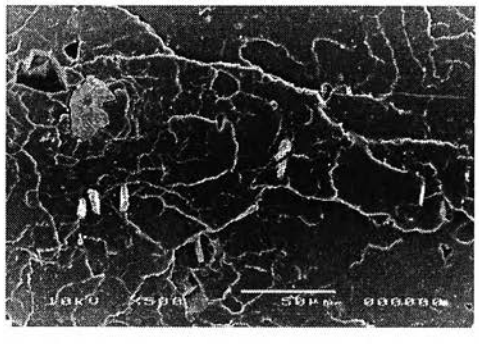

(e)

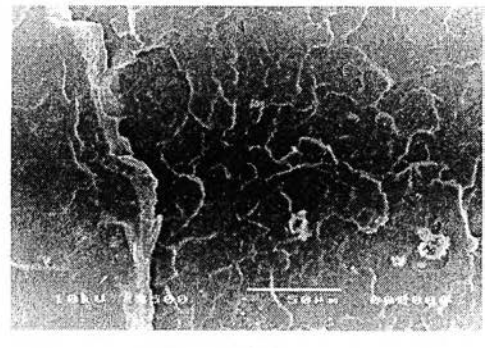

(f)

Figure 4

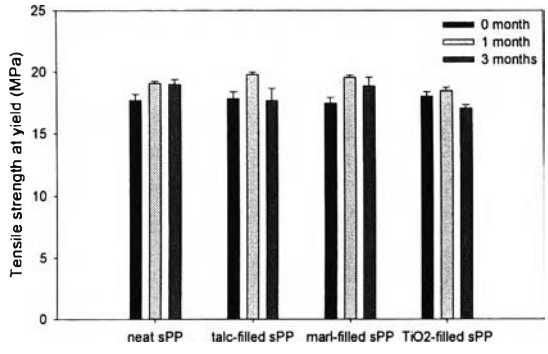

(a)

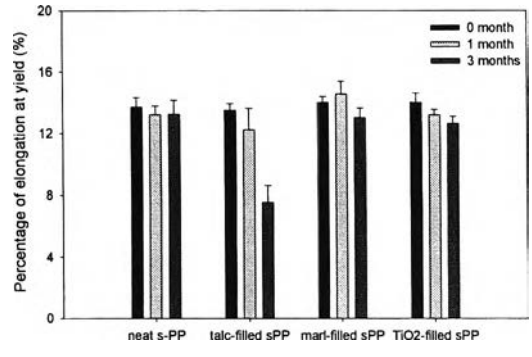

(b)

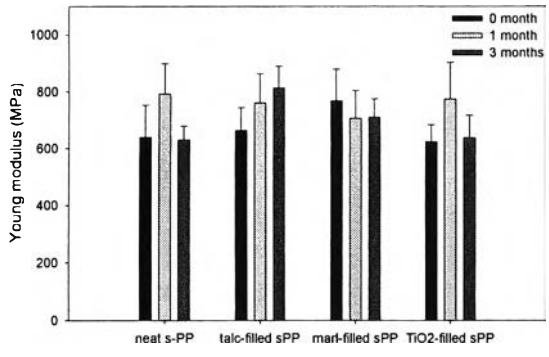

(c)

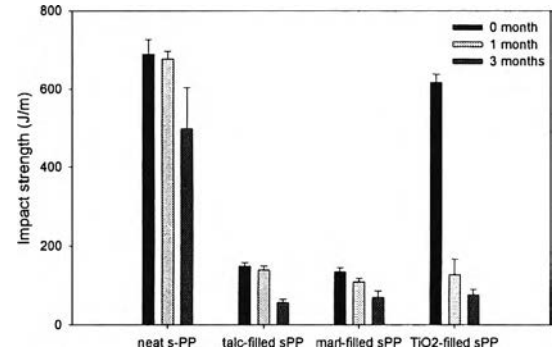

(d)

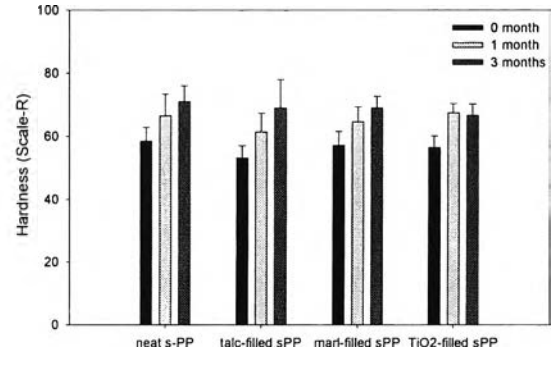

Figure 5